

## HARD-PHOTON PLUS GLUON JETS IN $e^+e^-$ COLLISIONS\*

S. MELJANAC

*Ruder Bošković Institute, P. O. B. 1016,  
41001 Zagreb, Croatia, Yugoslavia*

Received 26 October 1981

UDC 539.12

Original scientific paper

We discuss the possibility of producing direct photons plus two-gluon final states in  $e^+e^-$  collisions,  $e^+e^- \rightarrow \gamma + 2 \text{ gluons} \rightarrow \gamma + \text{hadrons}$ , both off and on the  $Z_0$  resonance. We have found that the background processes  $e^+e^- \rightarrow \gamma + q\bar{q} \rightarrow \gamma + \text{hadrons}$  dominate everywhere. Off the  $Z_0$  resonance, the ratio of distributions is smaller than  $10^{-3}$  for  $0.7 \lesssim x_\gamma \lesssim 0.9$  and decreases as  $x_\gamma \rightarrow 1$ , and is therefore unobservable at PETRA or PEP. On the  $Z_0$  resonance, we have estimated the ratio of distributions to be as large as  $\approx 10^{-3}$  for  $0.7 \lesssim x_\gamma \lesssim 0.9$  and found its upper limit to be  $\approx 0.1$  as  $x_\gamma \rightarrow 1$ .

### 1. Introduction

Recently the study of states made out of gluons has played an important role in elucidating a number of vital problems in QCD, such as the existence of bound glueball states, features of gluon fragmentation into hadrons, etc.<sup>1)</sup>

Hadrons that we find easy to access are essentially made out of quarks, and this makes it difficult to distinguish and identify gluonic final states in hadronic collisions. An interesting exception is provided by final states arising from the decay of bound states of pairs of heavy quarks (quarkonia)<sup>1)</sup>. In this case, owing to the Zweig rule, final hadrons arise from a pure three-gluon state, and study of, e. g.,  $\psi \rightarrow \gamma + \text{hadrons}$ , enables one to have access to two-gluon final states.

---

\* This work was supported by SIZ IV, Zagreb, Croatia, Yugoslavia

Recently much effort has been devoted to the investigation of photon-photon collisions<sup>2,3)</sup> and the production of gluonic jets in  $e^+e^-$  collisions in non-resonant regions. In the latter, processes with the production of three gluonic jets in the annihilation channel and with the production of two gluonic jets in the scattering channel have been investigated in the lowest order of electromagnetic and strong coupling constants<sup>4)</sup>.

In this paper we consider another reaction where a pure two-gluon final state is also possible, namely

$$e^+e^- \rightarrow \gamma + 2 \text{ gluons} \rightarrow \gamma + \text{hadrons.} \quad (1)$$

Reaction (1) proceeds through the diagrams shown in Fig. 1. It is obvious that the study of this reaction is of particular interest. In fact, when the energy of the photon approaches its kinematic limit, the two gluons have a small invariant mass

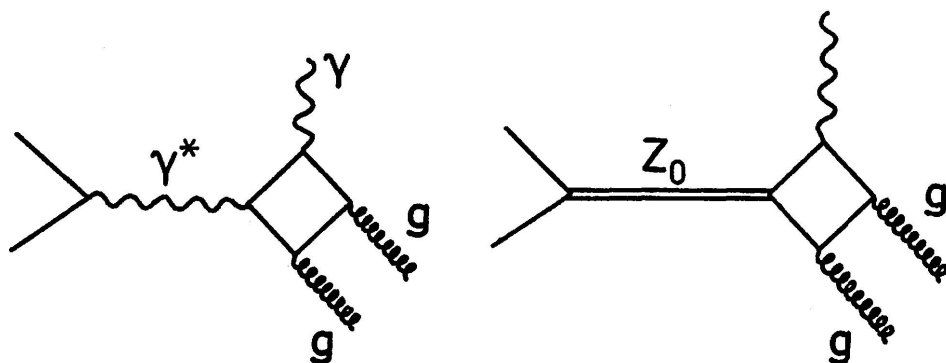


Fig. 1. Diagrams contributing to the process  $e^+e^- \rightarrow \gamma + 2 \text{ gluons}$ .

and could form (glueball) bound states. At energies which are not so high, gluon jets could be studied in isolation. The background, however, presents considerable difficulties. The final state, hard  $\gamma + \text{hadrons}$ , can also be produced by two other competing mechanisms:

- (i) quark bremsstrahlung (Figs. 2a,b);
- (ii) electron bremsstrahlung with the formation of a low-mass high-energy  $q\bar{q}$  pair (Figs. 2c,d).

Indeed, the problem is whether there are kinematic regions in the  $\gamma$  phase space where the diagrams of Fig. 1 dominate or at least give a sizable contribution to reaction (1).

The process shown in Fig. 2c is associated with serious difficulties because for small values of the invariant hadronic mass this process behaves as  $q^2/M^2$  (hadrons), while the two-gluon cross section is expected to behave at most as  $\ln^2(M_{g\bar{g}}^2/q^2)$ . The only possibility allowing for the suppression of this contribution is to go on top of the  $Z_0$  vector boson. In this case, the processes shown in Figs. 1b and 2b

would be enhanced with respect to the processes in Figs. 1a and 2a, c, d by the large ratio

$$[M_{Z_0}/\Gamma(Z_0 \rightarrow \text{all})]^2 \sim \frac{1}{\alpha^2}. \tag{2}$$

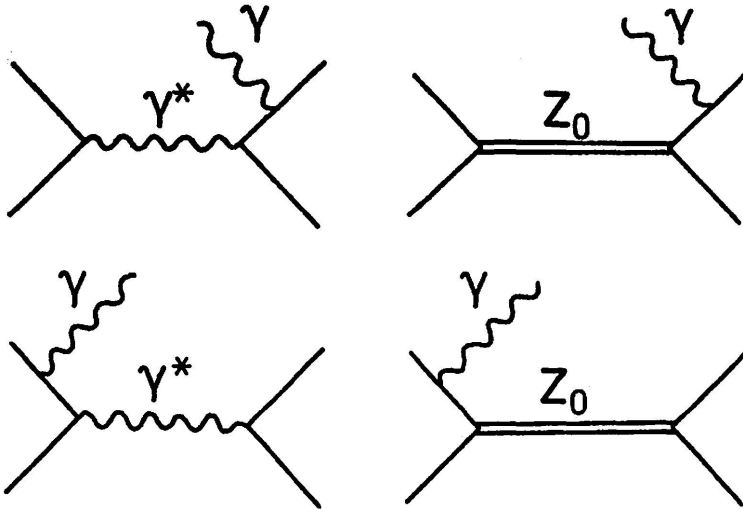


Fig. 2. Diagrams contributing to the background processes  $e^+e^- \rightarrow \gamma + q\bar{q}$ : (a) and (b) quark bremsstrahlung; (c) and (d) electron bremsstrahlung.

Thus, at the level of a qualitative estimate, the possibility of observing two-gluon states among the radiative decays of the  $Z_0$  resonance remains open, at least in certain kinematic regions <sup>5)</sup>.

We have found that in the reaction shown in Fig. 1 background reactions dominate both off and on the  $Z_0$  resonance in all kinematic regions. However, we cannot exclude the possibility that a better definition of hadronic final states could lead to a reduction in background such that reaction (1) would be observable.

The plan of the paper is as follows:

In Sect. 2 we present the lowest-order calculation of the differential cross section for the  $e^+e^- \rightarrow \gamma + 2g$  process in the standard  $SU(3) \times SU(2) \times U(1)$  model. We calculate the different angular distributions in terms of invariant quantities. In Sect. 3 we consider the background processes  $e^+e^- \rightarrow \gamma + q\bar{q}$ . In Sect. 4 we compare and discuss the results.

## 2. Calculations of the process $e^+e^- \rightarrow \gamma + 2$ gluons

The calculation of the process  $e^+e^- \rightarrow \gamma + 2$  gluons is performed in the lowest order of the standard  $SU(3) \times SU(2) \times U(1)$  model<sup>6,7)</sup>. The relevant diagrams are shown in Fig. 1. The process proceeds through the internal quark

loop. We take the limit  $m(\text{quark})/E \rightarrow 0$ , which is a good assumption for high-energy processes (at least for the first and second fermion generation). We note that there are no mass singularities<sup>8)</sup>. The structure of the loop-part diagram in Fig. 1a is the same as that computed in Ref. 9 in pure QED with an electron in the internal loop. (The only difference is the colour factor  $\frac{1}{4} \text{Tr } \lambda_a \lambda_b$ .) Furthermore, we note that the  $Z_0$  coupling to the quark loop is a pure vector since, in compliance with Furry's theorem, the axial-vector-coupling term cancels under charge-conjugation invariance. This implies that the structure of the loop-part diagram in Fig. 1b is the same as that in Fig. 1a (except the weak-interaction factors).

The scattering amplitude summed over quark flavours reads

$$\sum_{f=1}^{N_f} \frac{e^3 g_s^2}{2(2\pi)^2} \left[ \frac{Q_f^2}{q^2} I_\mu^{(1)} + \frac{Q_f (g_V)_f}{q^2 - M_R^2} I_\mu^{(2)} \right] G_{\mu f}^{\lambda_2 \lambda_3 \lambda_4} \text{Tr } \frac{\lambda_a}{2} \frac{\lambda_b}{2}, \tag{2.1}$$

where

$$I_\mu^{(1)} = \bar{u}(p_1) \gamma_\mu v(p_2),$$

$$I_\mu^{(2)} = \bar{u}(p_1) \gamma_\mu [(g_V)_e - (g_A)_e \gamma_5] v(p_2),$$

$$(g_V)_i = \frac{(T_3)_i - 2Q_i \sin^2 \Theta_W}{\sin 2\Theta_W}, \tag{2.2}$$

$$(g_A)_i = \frac{(T_3)_i}{\sin 2\Theta_W},$$

$$M_R^2 = M_Z^2 - iM_Z \Gamma.$$

Here,  $p_1$  ( $p_2$ ) is the four-momentum of  $e^-$  ( $e^+$ ) and  $q = p_1 + p_2$ . In CMS,  $p_1 = (E, \vec{p}_1)$ ,  $p_2 = (E, -\vec{p}_1)$  and  $q^2 = 4E^2$ .  $T_3$  is the third component of weak isospin,  $Q_W$  is the Weinberg angle,  $Q_f$  is the quark charge of flavour  $f$  (in units of proton charge),  $N_f$  is the number of flavours,  $M_Z$  is the mass of the  $Z_0$  boson and  $\Gamma$  is the total width of  $Z_0$  [ $\Gamma(Z_0 \rightarrow \text{all}) \sim 2.2$  GeV,  $M_Z \approx 90$  GeV]. The symbol  $G_{\mu f}^{\lambda_2 \lambda_3 \lambda_4}$  denotes the current of the heavy-photon decay into three photons through the internal  $f$ -quark loop; in the limit  $m_q/E \rightarrow 0$ , this current does not depend on flavour.

The differential cross section averaged over polarisation states of the initial  $e^+e^-$  beam and summed over colour states and final helicities is

$$d\sigma = \frac{\alpha^3 \alpha_s^2}{2(2\pi)^4 q^4} K (\delta_{ij} - n_i n_j) T_{ij} \delta^{(4)}(q - k_2 - k_3 - k_4) \cdot \frac{d^3 k_2 d^3 k_3 d^3 k_4}{k_{20} k_{30} k_{40}} \tag{2.3}$$

where

$$K = \left( \sum_{f=1}^{N_f} Q_f^2 \right)^2 + 2\eta \text{Re} \frac{q^2}{q^2 - M_R^2} + \kappa \left| \frac{q^2}{q^2 - M_R^2} \right|^2. \tag{2.4}$$

Here,

$$\eta = \left( \sum_{f=1}^{N_f} Q_f^2 \right) \left( \sum_{f=1}^{N_f} Q_f (g_V)_f (g_V)_e \right)$$

$$\varkappa = \left[ \sum_{f=1}^{N_f} Q_f (g_V)_f \right]^2 \cdot (g_V^2 + g_A^2)_e,$$

and  $\vec{n} = \vec{p}_1/E$  is the beam direction. The symbol  $k_2$  is the four-momentum of the photon and  $k_3$  and  $k_4$  are the four momenta of the gluons. The interference term is relatively small since  $(g_V)_e \sim 4 \sin^2 \theta_W - 1 \approx 0$ . We write the tensor  $T_{ij}$  in terms of four standard tensors which are built up of unit vectors  $\hat{k}_2$ , and  $\hat{k}_3$  ( $\delta_{ij}$  depends on these),

$$T_{ij} = G_1(234) (\hat{k}_3 - \hat{k}_2)_i (\hat{k}_3 - \hat{k}_2)_j + G_2(234) (\hat{k}_4 - \hat{k}_2)_i (\hat{k}_4 - \hat{k}_2)_j + \tag{2.5}$$

$$+ G_3(234) \cdot \frac{1}{2} [(\hat{k}_3 - \hat{k}_2)_i (\hat{k}_4 - \hat{k}_2)_j + (\hat{k}_3 - \hat{k}_2)_j (\hat{k}_4 - \hat{k}_2)_i] + G_4(234) \hat{N}_i \hat{N}_j,$$

where

$$\hat{N} = \frac{\vec{k}_2 \times \vec{k}_3}{|\vec{k}_2 \times \vec{k}_3|}.$$

The invariant quantities can be expressed in terms of four independent spiral amplitudes  $E_{\lambda_2 \lambda_3 \lambda_4}^{(i)}$  defined in Ref. 9. The invariants satisfy the following relations:

$$G_1(234) = G_1(432),$$

$$G_2(234) = G_1(243),$$

$$G_3(234) = G_3(243),$$

$$G_4(234) = G_4(243) = G_4(423). \tag{2.6}$$

Hence we are left only with three independent quantities, say  $G_1$ ,  $G_3$  and  $G_4$ , which we express explicitly in the Appendix.

Now, we can write different angular distributions using

$$\delta^{(4)}(q - k_2 - k_3 - k_4) \frac{d^3 k_2 d^3 k_3 d^3 k_4}{k_{20} k_{30} k_{40}} \rightarrow \frac{2\pi}{4} q^2 dx_2 dx_3 d\Omega_n^+, \tag{2.7}$$

where  $d\Omega_n^{\rightarrow}$  is the differential space angle of the initial beam (the  $e^-$  direction) related to the fixed production plane, and

$$x_i = \frac{k_{i0}}{E} \quad (i = 2,3,4), \tag{2.8}$$

$$x_2 + x_3 + x_4 = 2.$$

Hence

$$d\sigma = \frac{\alpha^3 \alpha_S^2}{8(2\pi)^3 q^2} K(\delta_{ij} - n_i n_j) T_{ij} dx_2 dx_3 d\Omega_n^{\rightarrow}. \tag{2.9}$$

First, the angular distribution in  $\Theta_2$ , where  $\Theta_2$  is the angle between the beam axis and the photon direction, is

$$\frac{d\sigma}{dx_2 dx_3 \cos \Theta_2} = \frac{\alpha^3 \alpha_S^2}{16(2\pi)^2 q^2} K \left[ \frac{A}{2} (1 + \cos^2 \Theta_2) + B \sin^2 \Theta_2 \right]. \tag{2.10}$$

Here,

$$A = \frac{4y_2 y_3 y_4}{x_2^2} \left[ \frac{G_1(234)}{x_3^2} + \frac{G_1(243)}{x_4^2} - \frac{G_3(234)}{x_3 x_4} \right] + G_4(234), \tag{2.11}$$

$$B = \frac{4}{x_2^2} \left[ \frac{y_4^2}{x_3^2} G_1(234) + \frac{y_3^2}{x_4^2} G_1(243) + \frac{y_3 y_4}{x_3 x_4} G_3(234) \right], \tag{2.12}$$

with  $Y_i = 1 - x_i$  ( $i = 2,3,4$ ).

Second, the angular distribution in  $\Theta$ , where  $\Theta$  is the angle between the beam direction and the normal of the production plane, is of the form

$$\frac{d\sigma}{dx_2 dx_3 d\cos\Theta} = \frac{\alpha^3 \alpha_S^2}{16(2\pi)^2 q^2} K \left[ \frac{C}{2} (1 + \cos^2 \Theta) + D \sin^2 \Theta \right], \tag{2.13}$$

where

$$C = \frac{4}{x_2} \left[ \frac{y_3}{x_2} G_1(234) + \frac{y_3}{x_4} G_1(243) + \frac{y_3 y_3}{x_3 x_4} G_3(234) \right] \tag{2.14}$$

$$D = G_4(234). \tag{2.15}$$

We write the quantities  $A$ ,  $B$ ,  $C$ , and  $D$  in two cases:

(a) at the centre of the Dalitz plot  $x_2 = x_3 = x_4 = \frac{2}{3}$ :

$$A = 16 \left[ 4 + \frac{27}{2} a^2 + 3b^2 \right] \approx 16 \cdot 15.2,$$

$$B = 16 \cdot \frac{27}{2} a^2 \approx 16 \cdot 3.3, \tag{2.16}$$

$$C = 16 \cdot 27a^2 \approx 16 \cdot 6.6,$$

$$D = 16 \cdot [4 + 3b^2] \approx 16 \cdot 11.9,$$

where

$$a = \frac{1}{3} - \frac{3}{2} \ln 3 - \frac{2}{3} \left[ \frac{\pi^2}{6} + 2\Phi\left(\frac{2}{3}\right) - \ln^2 3 \right] \approx -0.49,$$

$$b = -3 \ln 3 - 4 \left[ \frac{\pi^2}{6} + 2\Phi\left(\frac{2}{3}\right) - \ln^2 3 \right] \approx 1.62,$$

with the Spence function,

$$\Phi(Z) = \int_0^Z \frac{\ln|1-t|}{t} dt; \tag{2.17}$$

(b) in the limit  $x_2 \rightarrow 1, x_3 \sim x_4 \sim \frac{1}{2}$

$$A = 16 \left\{ 4 + 2 \left[ Z_1^2 + \frac{y_3^2}{x_3^2} Z_2^2 + \frac{x_3^2}{y_3^2} Z_3^2 \right] \right\},$$

$$B \approx 0,$$

$$C = 16 \left\{ Z_1^2 + \frac{y_3^2}{x_3^2} Z_2^2 + \frac{x_3^2}{y_3^2} Z_3^2 \right\} = \frac{1}{2} A - 32, \tag{2.18}$$

$$D = 16 \left\{ 4 + Z_1^2 + \frac{y_3^2}{x_3^2} Z_2^2 + \frac{x_3^2}{y_3^2} Z_3^2 \right\} = \frac{1}{2} A + 32,$$

where

$$Z_1 = 1 + \frac{\ln x_3}{y_3} + \frac{\ln y_3}{x_3},$$

$$Z_2 = -(1 + \ln y_2) \ln y_3 + \varphi(x_3),$$

$$Z_3 = -(1 + \ln y_2) \ln x_3 + \varphi(y_3).$$

In this limit, the integration over  $x_3$  gives (for  $x_2 \rightarrow 1$ )

$$\tilde{A}(x_2) \approx \int_{y_2}^1 \frac{A}{16} dx = 8(1 + \zeta_2 - 2\zeta_3) \ln^2(1 - x_2) +$$

$$+ 8(5 - \zeta_2 - 5\zeta_3 + \zeta_2^2) \ln(1 - x_2) + 8\left(\frac{31}{4} - \zeta_2 - 5\zeta_3 + \zeta_2^2 - 2\zeta_2\zeta_3 + 3\zeta_3\right) \approx 1.93 \ln^2(1 - x_2) + 0.4 \ln(1 - x_2) + 16,$$

$$\tilde{B}(x_2) \approx \int_{y_2}^1 \frac{B}{16} dx_3 = O(y_2), \tag{2.19}$$

$$\tilde{C}(x_2) \approx \int_{y_2}^1 \frac{C}{16} dx_3 = \frac{1}{2} A(x_2) - 2,$$

$$\tilde{D}(x_2) \approx \int_{y_2}^1 \frac{D}{16} dx_3 = \frac{1}{2} A(x_2) + 2.$$

Since the angular distributions exhibit a behaviour similar to that of the analogous distributions for the background process (Sect. 3), kinematics cannot be used to separate gluon jets from quark jets. Therefore, we can integrate over angles without loss of some useful information and the result is

$$\frac{d\sigma}{dx_2 dx_3} = \frac{a^3 a_s^2 K}{12 (2\pi)^2 q^2} (A + B). \tag{2.20}$$

Here,  $A + B = C + D$  can be put in the following symmetric form:

$$A + B = 16[S(234) + S(324) + S(423)], \tag{2.21}$$

where

$$S(234) = S_1(234) + S_2(234),$$

as given in the Appendix.

The distribution (2.20) has a minimum at the centre of the Dalitz plot and then it grows up to the boundary of the Dalitz plot. The integration over  $x_3$  gives

$$\frac{d\sigma}{dx_2} = \frac{2a^3 a_s^2 K}{3\pi^2 q^2} F(x_2), \tag{2.22}$$

where the function  $F(x_2)$  is shown in Fig. 3<sup>4)</sup>. The approximative expressions for  $F(x_2)$  are very simple in the limits  $x_2 \ll 1$  and  $(1 - x_2) \ll 1$ :

$$F(x_2) \approx 4x_2 (\ln^2 x_2 - 2 \ln x_2 + 3), \quad x_2 \ll 1,$$

$$F(x_2) \approx 1.93 \ln^2(1 - x_2) + 0.4 \ln(1 - x_2) + 16, \quad (1 - x_2) \ll 1. \tag{2.23}$$

We note that

$$\int_0^1 F(x_2) dx_2 \approx 15 \tag{2.24}$$

and the total cross section is

$$\sigma \approx \frac{10^{-6} K}{2q^2 (\text{GeV})^2 \ln^2 \frac{q^2}{A^2}} \text{ mb}, \tag{2.25}$$

where  $K$  is defined in (2.4).

For example, for  $q^2 \approx M_Z^2$  and also for  $q_2 \approx 100 \text{ GeV}^2$ , the total cross section is roughly  $\sigma \simeq 3 \times 10^{-10} \text{ mb}$ .

### 3. Background processes

Background processes for reaction (1) are provided by all processes in which the final states consist of a hard photon + hadrons (not coming from the two-gluon configuration):

- (i) quark bremsstrahlung (Figs. 2a, b);
- (ii) electron bremsstrahlung (Figs. 2c, d);
- (iii) photons coming from  $\pi^0$  decays.

These processes were discussed in Ref. 10; it was shown that there existed a kinematic region where contribution (i) dominated for values of  $x_2$  which were not too large ( $0.5 \lesssim x_2 \lesssim 0.8$ ).

We are especially interested in the limit  $x_2 \rightarrow 1$  since the process in Fig. 1 gives the largest contribution on the boundary of the Dalitz plot. Therefore, we study the behaviour of the background processes in this limit. In any case, the perturbative treatment is not allowed (valid) in the region where  $x_2$  is too close to 1. Unfortunately, the contribution from the diagram (c) in Fig. 2 behaves as  $1/q_2 (1 - x_2) = 1/M_{qq}^2 = 1/M_{gg}^2$  when  $x_2 \rightarrow 1$  and the process in Fig. 1 is irrelevant because the ratio  $d\sigma/d\sigma_{\text{background}} \sim M_{gg}^2/q^2 \ln^2 M_{gg}^2/q^2$  tends towards zero when  $M_{gg}^2/q^2$  approaches zero.

In order to avoid the contribution coming from Fig. 2c, we go on top of the  $Z_0$  vector. In this case, we consider the dominant contribution coming from Fig. 2b. We also note that contribution (iii) decreases logarithmically for  $x_2 \rightarrow 1^{(10)}$ , and contribution (i) is dominant.

The calculation of quark bremsstrahlung is performed in the lowest order of perturbation theory, and we suppose that  $m_q/M_Z \ll 1$  for every quark flavour. The differential cross section averaged over the polarisation states of the initial  $e^+e^-$  beam and summed over colour states and final helicities is

$$d\sigma = \frac{3\alpha^3}{16 \pi^2 q^2} [K' (\delta_{ij} - n_i n_j) l_{ij}^{(\alpha)} + K'' a_{\mu\nu}^{(\alpha)} a_{\mu\nu}^{(\alpha)}], \tag{3.1}$$

$$\times \delta^{(4)}(q - k_2 - k_3 - k_4) \frac{d^3 k_2 d^3 k_3 d^3 k_4}{k_{20} k_{30} k_{40}}$$

Here,

$$\begin{aligned}
 K' &= (g_V^2 + g_A^2)_e \left| \frac{q^2}{q^2 - M_R^2} \right|^2 \sum_{f=1}^{N_f} Q_f^2 (g_V^2 + g_A^2)_f, \\
 K'' &= 4 (g_V g_A)_e \left| \frac{q_2}{q^2 - M_R^2} \right|^2 \sum_{f=1}^{N_f} Q_f^2 (g_V g_A)_f,
 \end{aligned}
 \tag{3.2}$$

$k_2$  is the four-momentum of the photon and  $k_3$  ( $k_4$ ) is the four-momentum of the quark (antiquark). We neglect the term  $K''$  because ratio  $K''/K'$  is proportional to  $(g_V/g_A)_e = 1 - 4 \sin^2 \Theta_W \approx 0.1$ . The term  $K''$  drops out automatically after the phase-space integration because  $a_{ij}^{(q)}$  is antisymmetric under the change  $k_3 \leftrightarrow \bar{k}_4$ , whereas the phase-space integration is symmetric.

We write the tensor  $l_{ij}^{(q)}$  in the form

$$\begin{aligned}
 l_{ij}^{(q)} &= L_0 \delta_{ij} + L_1 \hat{k}_{3i} \hat{k}_{3j} + L_2 \hat{k}_{4i} \hat{k}_{4j} + L_3 \frac{1}{2} (\hat{k}_{3i} \hat{k}_{4j} + \hat{k}_{3j} \hat{k}_{4i}) + \\
 &+ L_4 \frac{1}{2} (\hat{k}_{2i} \hat{k}_{3j} + \hat{k}_{2j} \hat{k}_{3i}) + L_5 \frac{1}{2} (\hat{k}_{2i} \hat{k}_{4j} + \hat{k}_{2j} \hat{k}_{4i}).
 \end{aligned}
 \tag{3.3}$$

Here,

$$\begin{aligned}
 \hat{k}_i &= \frac{\vec{k}_i}{|\vec{k}_i|}, \quad (i = 2,3,4), \\
 L_0 &= 4 \frac{x_3^2 + x_4^2}{(1-x_3)(1-x_4)}, \quad L_3 = 4 \frac{(x_3 + x_4) x_3 x_4}{(1-x_3)(1-x_4)}, \\
 L_1(3,4) &= -\frac{4x_3^2}{1-x_3}, \quad L_2(3,4) = L_1(4,3), \\
 L_4(3,4) &= \frac{4x_3^2 x_2}{(1-x_3)(1-x_4)}, \quad L_5(3,4) = L_4(4,3),
 \end{aligned}
 \tag{3.4}$$

and the following relation holds:

$$L_1 + L_2 + L_2 \cos \beta_{34} + L_4 \cos \beta_{23} + L_5 \cos \beta_{24} = -L_0,
 \tag{3.5}$$

where  $\cos \beta_{23} = 1 - 2(1-x_4)/x_2 x_3$ , etc.

Now we write angular distributions analogous to those given by (2.10) and (2.13)

First, the angular distribution in  $\Theta_2$ , where  $\Theta_2$  is the angle between the beam axis and the photon direction, is

$$\frac{d\sigma}{dx_2 dx_3 d \cos \Theta_2} = \frac{3\alpha^3}{16q^2} K' \left[ \frac{A'}{2} (1 + \cos^2 \Theta_2) + B' \sin^2 \Theta_2 \right],
 \tag{3.6}$$

where

$$A' = 8 \left[ \frac{x_3^2 + x_4^2}{(1-x_3)(1-x_4)} - \frac{4(1-x_2)}{x_2^2} \right],$$

$$B' = 8 \frac{4(1-x_2)}{x_2^2}. \quad (3.7)$$

In this case, the  $K''$  term drops out automatically after the azimuthal integration around the  $\hat{k}_2$  direction.

Second, the angular distribution in  $\Theta$ , where  $\Theta$  is the angle between the beam axis and the normal of the production plane, is

$$\frac{d\sigma}{dx_2 dx_3 d \cos \Theta} \approx \frac{3\alpha^3}{16q^2} K' \left[ \frac{1}{2}(1 + \cos^2 \Theta) + \sin^2 \Theta \right] \cdot C', \quad (3.8)$$

where

$$C' = 4 \frac{x_3^2 + x_4^2}{(1-x_3)(1-x_4)}. \quad (3.9)$$

We write the quantities  $A'$ ,  $B'$ , and  $C'$  in two cases:

(a) at the centre of the Dalitz plot  $x_2 = x_3 = x_4 = \frac{2}{3}$ :

$$A' = 40,$$

$$B' = 24, \quad (3.10)$$

$$C' = 32;$$

(b) in the limit  $x_2 \rightarrow 1, x_3 \approx x_4 \approx \frac{1}{2}$ :

$$A' = 8 \frac{x_3^2 + x_4^2}{(1-x_3)(1-x_4)},$$

$$B' = O(y_2), \quad (3.11)$$

$$C' = 4 \frac{x_3^2 + x_4^2}{(1-x_3)(1-x_4)}.$$

In case (b), the integration over  $x_3$  gives ( $x_2 \rightarrow 1$ )

$$\begin{aligned} \tilde{A}'(x_2) &\approx 16 \frac{1 + (1 - x_2)^2}{x_2} \ln(1 - x_2) \frac{q^2}{\Lambda^2}, \\ \tilde{B}'(x_2) &\approx O(y_2), \end{aligned} \tag{3.12}$$

$$\tilde{C}'(x_2) \approx 8 \cdot \frac{1 + (1 - x_2)^2}{x_2} \ln(1 - x_2) \frac{q^2}{\Lambda^2},$$

where  $\Lambda$  is the scale parametar ( $\Lambda_{QCD} \approx 0.4$  GeV).

For heavy quarks, we should make the replacement  $\Lambda \rightarrow m_q$  since the actual parametar is an effective quark mass.

Our results are not applicable to the events where  $M_{qq}^2 = (1 - x_2)q^2$  is small, i. e.  $x_2$  is very close to 1. Nevertheless, we will use these results for  $M_Z^2 \gg M_{qq}^2 \gg \Lambda^2$  to make at least a qualitative comparison with the analogous results for reaction (1) (Fig. 1). The integration over angles in (3.6) or (3.7) gives

$$\frac{d\sigma}{dx_2 dx_3} = \frac{2\alpha^3}{q^2} K' \frac{x_3^2 + x_4^2}{(1 - x_3)(1 - x_4)}. \tag{3.13}$$

This distribution has a minimum for  $x_2 \approx 1, x_3 \approx x_4 \approx \frac{1}{2}$ .

Finally, the integration over  $x_3$  gives

$$\frac{d\sigma}{dx_2} = \frac{4\alpha^3 K'}{q^2} \cdot \frac{1 + (1 - x_2)^2}{x_2} \ln \frac{M_{qq}^2}{\Lambda^2}, \tag{3.14}$$

where  $M_{qq}^2 = (1 - x_2)q^2$  and  $q^2 = M_Z^2$ .

To conclude this section, we wish to mention that the angular distribution in  $\Theta_2$  coming from Fig. 2c is

$$\frac{d\sigma}{dx_2 dx_3 d \cos \Theta_2} = \frac{3\alpha^3}{16q^2} \left( \sum_{f=1}^{N_f} Q_f^2 \right) \frac{\left[ \frac{A'}{2}(1 + \cos^2 \Theta_2) + B' \sin^2 \Theta_2 \right] (1 - x_3)(1 - x_4)}{x_2^2 (1 - x_2) \sin^2 \Theta_2},$$

where  $A'$  and  $B'$  are given by (3.7).

#### 4. Comparison of results and conclusions

We now compare the result for the process in Fig. 1 with that for the process in Fig. 2 on top of the  $Z_0$  vector boson. To make a rough estimate, we suppose that  $N_f = 6$ ,  $M_Z \approx 100$  GeV and  $\Lambda \approx 0.4$  GeV. Then we have

$$\frac{K}{K'} = \frac{\left[ \sum_f Q_f (g_V)_f \right]^2}{\sum_f Q_f^2 (g_V^2 + g_A^2)_f} \approx N_{\text{doublet}} \cdot 0.3 \approx 1, \tag{4.1}$$

$$\alpha_S = \frac{4\pi}{11 - \frac{2}{3} N_f} \cdot \frac{1}{\ln \frac{M_Z^2}{\Lambda^2}} \approx 0.18.$$

(a) At the centre of the Dalitz plot, the ratios of (2.10), (2.13) and (2.20) to (3.6), (3.8) and (3.12), respectively, are

$$\begin{aligned} & \left( \frac{d\sigma}{dx_2 dx_3 d \cos \Theta_2} \right) \Bigg| \left( \frac{d\sigma}{dx_2 dx_3 d \cos \Theta_2} \right)_{\text{background}} \approx \\ & \approx \left( \frac{d\sigma}{dx_2 dx_3 d \cos \Theta} \right) \Bigg| \left( \frac{d\sigma}{dx_2 dx_3 d \cos \Theta} \right)_{\text{background}} \approx \\ & \approx \left( \frac{d\sigma}{dx_2 dx_3} \right) \Bigg| \left( \frac{d\sigma}{dx_2 dx_3} \right)_{\text{background}} \approx \frac{\alpha_S^2}{(2\pi)^2} \frac{K}{K'} \frac{3}{2} \approx 10^{-3}. \end{aligned} \tag{4.2}$$

(b) In the limit  $x_2 \rightarrow 1$ ,  $x_3 \approx x_4 \approx \frac{1}{2}$ , the ratios of (2.10), (2.13) and (2.20) to (3.6), (3.8) and (3.12), respectively, are as follows:

$$\begin{aligned} & \left( \frac{d\sigma}{dx_2 dx_3 d \cos \Theta_2} \right) \Bigg| \left( \frac{d\sigma}{dx_2 dx_3 d \cos \Theta_2} \right)_{\text{background}} \approx \\ & \approx \left( \frac{d\sigma}{dx_2 dx_3 d \cos \Theta} \right) \Bigg| \left( \frac{d\sigma}{dx_2 dx_3 d \cos \Theta} \right)_{\text{background}} \approx \\ & \approx \left( \frac{d\sigma}{dx_2 dx_3} \right) \Bigg| \left( \frac{d\sigma}{dx_2 dx_3} \right)_{\text{background}} \approx \\ & \approx \frac{1}{6} \frac{K}{K'} \left[ \frac{\alpha_S}{\pi} \ln(1 - x_2) \right]^2 < \frac{1}{6} \frac{K}{K'} \left[ \frac{\alpha_S}{\pi} \ln \frac{M_Z^2}{\Lambda^2} \right]^2 \lesssim 0.1. \end{aligned} \tag{4.3}$$

(c) In the limit  $x_2 \rightarrow 1$ , the ratio of (2.22) to (3.14) is

$$R = \left( \frac{d\sigma}{dx_2} \right) \bigg/ \left( \frac{d\sigma}{dx_2} \right)_{background} = \left( \frac{\alpha_s}{2\pi} \right)^2 \frac{2}{3} \frac{K}{K'} \frac{\ln^2(1-x_2)}{\ln \frac{M_{qq}^2}{\Lambda^2}}$$

If we set  $M_{qq}^2/\Lambda^2 = \kappa \gg 1$ , but  $\ln \kappa \sim 1$ , we obtain the ratio

$$R < \left[ \frac{\alpha_s}{2\pi} \ln \frac{1}{\kappa} \frac{q^2}{\Lambda^2} \right]^2 \lesssim 0.1, \tag{4.4}$$

and for  $0.7 \lesssim x_2 \lesssim 0.9$ , we have

$$R \approx \left( \frac{\alpha_s}{2\pi} \right)^2 \sim 10^{-3}.$$

In fact, this ratio can be regarded as a function of the unknown quark mass  $m_t$ . We have not investigated this possibility, but we expect no dramatic change in the results.

In this paper we have studied the process  $e^+e^- \rightarrow \gamma + 2 \text{ gluons} \rightarrow \gamma + \text{hadrons}$  as a possible source of pure two-gluon final states. Calculating in the lowest order of the standard  $SU(3) \times SU(2) \times U(1)$  model and setting  $m_q = 0$  for all quark flavours, we have arrived at the following conclusions:

(i) The electron-bremsstrahlung process behaves as  $1/(1-x_2)$  for  $x_2 \rightarrow 1$  and is the dominant contribution to the process  $e^+e^- \rightarrow \text{hard } \gamma + \text{hadrons}$  (in this region). The ratio of the different distributions for reaction (1) to the analogous distributions for the background process is smaller than  $10^{-3}$  for  $0.5 \lesssim x_2 \lesssim 0.9$ , and even decreases as  $x_2$  approaches 1.

(ii) Since reaction (1) gives the largest contribution on the boundary of the Dalitz plot (i. e.  $x_2 \rightarrow 1$ ), the only possibility allowing for the suppression of the electron bremsstrahlung contribution is to go on top of the  $Z_0$  vector boson.

(iii) Kinematics cannot be used to separate gluon jets from quark jets since the angular distributions exhibit a similar behaviour.

(iv) The different distribution ratios for reaction (1) to the background reaction have been estimated to be  $10^{-3}$  for  $0.7 \lesssim x_2 \lesssim 0.9$ . For  $x_2 \rightarrow 1$ , the upper limit has been found to be  $R \lesssim 0.1$ . In any case, reaction (1) is dominated everywhere by background reactions. The estimate of the background is performed under the (pessimistic) assumption that no distinction is possible between a two-gluon jet and a  $q\bar{q}$  jet. Should one find a difference (in average multiplicities, etc.), the estimate of the background could be reduced, even drastically, since one could select events so that the  $g-g$  component would be enriched.

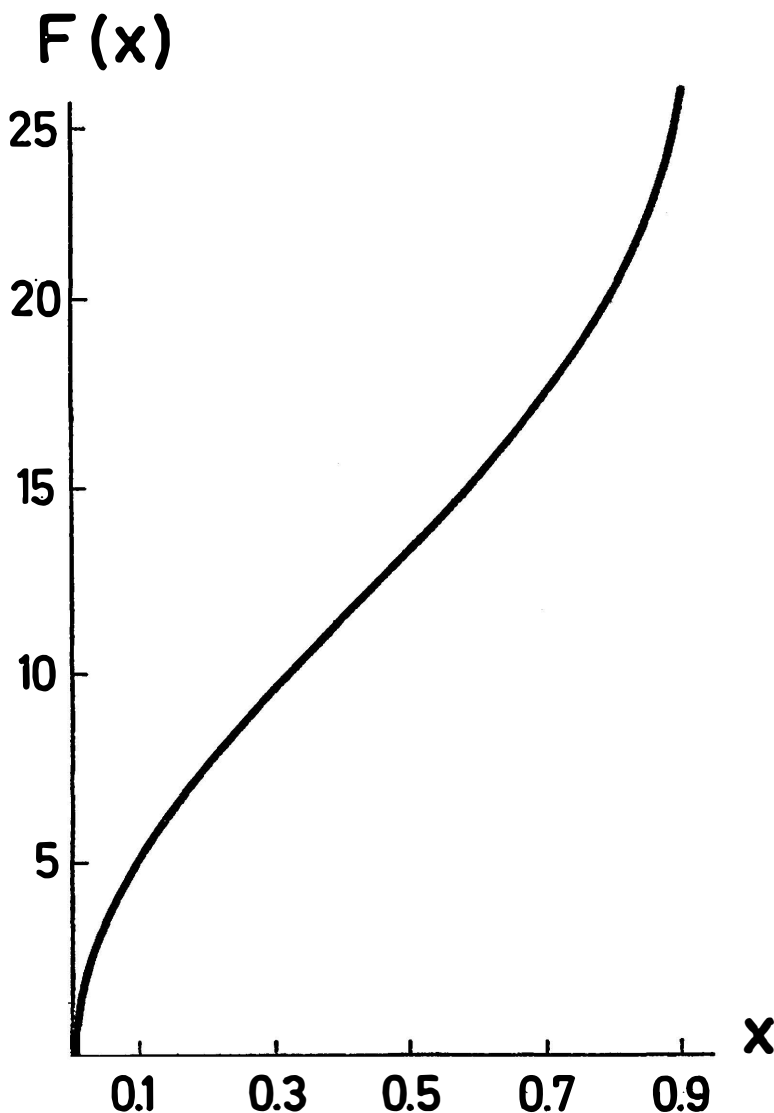


Fig. 3. Plot of the function  $F(x)$  in the limit  $m/E \rightarrow 0$ .

#### Acknowledgments

The author wishes to thank Prof. L. Maiani for suggesting the problem and persistent help during this work. It is also a pleasure to thank Profs. G. Altarelli and N. Cabibbo for valuable discussions and B. De Tollis for many useful conversations and encouragement during this work. The author also wishes to thank Istituto di Fisica Guglielmo Marconi, Rome, where this work was done, for its warm hospitality.

*Appendix*

In the limit  $m_q/E \rightarrow 0$ , the invariant quantities are the following:

$$\begin{aligned}
 G_1(234) &= G_1(432) = \\
 &= \frac{4y_3}{y_2 y_4} \left\{ \left[ 2y_4 + \left( \frac{2y_3 y_4}{y_2} + \frac{2y_4}{x_3} - y_3 \right) \ln y_3 + x_3 y_4 \left( \frac{2}{y_2} + \frac{1}{x_4} \right) \ln y_4 + \right. \right. \\
 &\quad \left. \left. + x_3 \left( \frac{2(y_3 - y_4)}{y_2} - \frac{4y_3 y_4}{y_2^2} \right) \tilde{T}(3,4) \right]^2 + [2 \leftrightarrow 4]^2 + \right. \\
 &\quad \left. + \left[ x_3 \left( \frac{y_2}{x_2} \ln y_2 - \frac{y_4}{x_4} \ln y_4 \right) + \frac{2x_3}{y_3} (y_4 - y_2) \tilde{T}(2,4) \right]^2 \right\}, \quad (A.1)
 \end{aligned}$$

$$\begin{aligned}
 G_3(234) &= G_3(243) = \\
 &= -\frac{8}{y_2} \left\{ \left[ 2y_2 + \left( \frac{2y_2 y_3}{y_4} + \frac{2y_2}{x_3} - y_3 \right) \ln y_3 + x_3 y_2 \left( \frac{2}{y_4} + \frac{1}{x_2} \right) \ln y_2 + \right. \right. \\
 &\quad \left. \left. + \left( \frac{2x_3 (y_3 - y_2)}{y_4} - \frac{4x_3 y_3 y_2}{y_4^2} \right) \tilde{T}(2,3) \right] \times \left[ \frac{x_4}{x_2} y_2 \ln y_2 - \frac{x_4}{x_3} y_3 \ln y_3 + \right. \right. \\
 &\quad \left. \left. + \frac{2x_4 (y_3 - y_2)}{y_4} \tilde{T}(2,3) \right] + [3 \leftrightarrow 4] \times [3 \leftrightarrow 4] + \right. \\
 &\quad \left. + \left[ 2y_4 + \left( \frac{2y_3 y_4}{y_2} + \frac{2y_4}{x_3} - y_3 \right) \ln y_3 + x_3 y_4 \left( \frac{2}{y_2} + \frac{1}{x_4} \right) \ln y_4 + \right. \right. \\
 &\quad \left. \left. + \left( \frac{2x_3 (y_3 - y_4)}{y_2} - \frac{4x_3 y_3 y_4}{y_2^2} \right) \tilde{T}(3,4) \right] \times [3 \leftrightarrow 4] \right\}. \quad (A.2)
 \end{aligned}$$

Here,

$$\tilde{T}(3,4) \approx \frac{1}{2} \left[ \frac{\pi^2}{6} + \Phi(x_3) + \Phi(x_4) - \ln y_3 \ln y_4 \right], \quad (A.3)$$

where  $\Phi(z)$  is the Spence (dilogarithmic) function,

$$\Phi(z) = \int_0^z dt \frac{\ln|1-t|}{t}.$$

The following relation is fully symmetric:

$$\frac{4}{x_2} \left[ \frac{y_4}{x_3} G_1(234) + \frac{y_3}{x_4} G_1(243) + \frac{y_3 y_4}{x_3 x_4} G_3(234) \right] =$$

$$= 16 [S_1(234) + S_1(324) + S_1(423)], \quad (\text{A.4})$$

where

$$S_1(234) = S_1(243) =$$

$$= \frac{1}{x_2^2} \left\{ \frac{2y_3 y_4}{x_3 x_4} (1 + y_2) + \frac{y_3}{x_3} \left( \frac{2y_4}{y_2} + \frac{2y_4}{x_3} + x_3 - x_4 \right) \ln y_3 + \right.$$

$$+ \frac{y_4}{x_4} \left[ \frac{2y_3}{y_2} + \frac{2y_3}{x_4} + x_3 - x_3 \right] \ln y_4 + \frac{2}{y_2^2} [y_2 (y_3 - y_4)^2 - 2x_2 y_3 y_4] \tilde{T}(3,4) \left. \right\}^2 +$$

$$+ \frac{y_3 y_4}{y_2 x_2^2} \left\{ \frac{2(y_4 - y_3) y_2}{x_3 x_4} + \frac{2}{x_3^2} (y_4 - 2y_3 x_3) \ln y_3 - \frac{2}{x_4^2} (y_3 - 2y_4 x_4) \ln y_4 + \right.$$

$$\left. + \frac{4(y_3 - y_4)}{y_2} \tilde{T}(3,4) \right\}^2. \quad (\text{A.5})$$

The quantity  $G_4(234)$  is fully symmetric, and can be put in the form

$$G_4(234) = 16 [S_2(234) + S_2(324) + S_2(423)], \quad (\text{A.6})$$

where

$$S_2(234) = S_2(243) = \frac{4}{3} +$$

$$+ \left[ \frac{y_3}{y_2 x_3} (2x_3 - y_2) \ln y_3 + \frac{y_4}{y_2 x_4} (2x_4 - y_2) \ln y_4 - \right.$$

$$\left. - \left( \frac{2x_2}{y_2} + \frac{4y_3 y_4}{y_2^2} \right) \tilde{T}(3,4) \right]^2.$$

#### References

- 1) P. Roy, Rutherford Laboratory preprint RL-80-007 (1980); D. S. Narayan, Models for Hadronization of Quarks and Gluons. Talk presented at X International Symposium on Multiparticle Dynamics, Goa, September 25-29, 1979;
- 2) J. F. Gunion, Preprint SLAC-PUB-2503, May 1980 (T/E);
- 3) P. V. Landshoff, Summary talk at the 4th International Colloquium on Photon-Photon Interactions, University of Paris, April 1981;
- 4) V. N. Bayer, E. A. Kuraev, V. S. Fadin, J. Nucl. Phys. **31** (1980) 700;

- 5) M. L. Laursen, K. O. Mikaelian and M. A. Samuel, Phys. Rev. **D23** (1981) 2795;
- 6) S. Weinberg, Phys. Rev. Lett. **19** (1967) 1264; Phys. Rev. **D5** (1972) 1412;  
A. Salam, in *Elementary Particle Theory: Relativistic Groups and Analyticity*; Nobel Symposium No. 8, Ed. by N. Svartholm, Almquist and Wicksell, Stockholm 1968, p. 367;
- 7) H. D. Politzer, Phys. Rep. **14C** (1974) 129;  
W. Marciano and H. Pagels, Phys. Rep. **36C** (1978) 137;
- 8) T. D. Lee and M. Nauenberg, Phys. Rev. **133B** (1964) 1549;
- 9) V. Constantini, B. De Tollis and G. Pistoni, *Nuovo Cimento* **2A** (1971) 733;
- 10) K. Koller, T. F. Walsh and P. Zerwas, Z. Phys. **C2** (1979) 197.

MLAZEVI TVRDIH FOTONA I GLUONA U SUDARIMA  $e^+e^-$

S. MELJANAC

*Institut »Ruđer Bošković«, 41001 Zagreb*

UDK 539.12

Originalni znanstveni rad

Razmatra se mogućnost produkcije direktnih fotona i konačnih stanja s dva gluona u sudarima  $e^+e^-$ ,  $e^+e^- \rightarrow \gamma + 2$  gluona  $\rightarrow \gamma +$  hadroni, kako izvan tako i na rezonanci  $Z_0$ . Nađeno je da su pozadinski procesi  $e^+e^- \rightarrow \gamma + q\bar{q} \rightarrow \gamma +$  hadroni svugdje dominantni. Izvan rezonance, omjer raspodjela je manji od  $10^{-3}$  za  $0.7 \lesssim x_\gamma \lesssim 0.9$  i opada kada se  $x$  približava jedinici, pa se zbog toga ne može opaziti na PETRA ili PEP. Na rezonanci, omjer raspodjela je procijenjen na  $\approx 10^{-3}$  za  $0.7 \lesssim x_\gamma \lesssim 0.9$ , te je nađeno da gornja granica iznosi  $\approx 0.1$  za  $x_\gamma \rightarrow 1$ .